Energetics of Metal−Ligand Multiple Bonds. A Combined Solution Thermochemical and ab Initio Quantum Chemical Study of M═O Bonding in Group 6 Metallocene Oxo Complexes

Lubin Luo,[†] Giuseppe Lanza,[‡] Ignazio L. Fragalà,*[,⊥] Charlotte L. Stern,[†] and Tobin J. Marks*[,†]

Contribution from the Department of Chemistry, Northwestern University, Evanston, Illinois 60208-3113, Dipartimento di Chimica, Università della Basilicata, 85100 Potentza, Italy, and Dipartimento di Scienze Chimiche, Università di Catania, 95125 Catania, Italy

Received March 31, 1997. Revised Manuscript Received November 2, 1997

Abstract: In this paper, we report a synthetic, molecular structure, thermochemical, and ab initio Hartree−Fock/Moller−Plesset level study of bonding and bonding energetics in the group 6 metallocene oxo series $Cp_2Mo/(MeCp)_2MO$, M = Cr, Mo, W. Efficient, high-yield syntheses of the pairs $Cp_2MH_2/(MeCp)_2MH_2$, $Cp_2MCl_2/(MeCp)_2MCl_2$, and $Cp_2MO/(MeCp)_2MO$ where M = Mo or W are reported. The molecular structure of $(MeCp)_2WO$ features a "bent sandwich" geometry with a W═O distance of 2.04(1) Å and an average W−C(Cp) distance of 2.371(8) Å. Thus, W−C(Cp) exhibits a ∼0.07 Å elongation over the corresponding distance in typical Cp_2WX_2 complexes and a W═O distance which appears to be elongated versus what might be expected for a formal triple bond. D(M═O) values obtained from $(MeCp)_2MO$ silanolytic (Me_3SiCl, Me_3SiI) batch titration calorimetry are very large: 110(11) kcal/mol (M = Mo) and 132(10) kcal/mol (M = W). The corresponding D(W−OTMS) value is determined to be 65(18) kcal/mol. Ab initio relativistic core potential calculations reveal significantly weakened M−Cp bonding versus that in the corresponding Cp_2MCl_2 compounds, weakened M═O bonding due to population of M−O π antibonding levels, and a pronounced accumulation of negative charge on the oxo ligand (consistent with observed nucleophilicity of these complexes). Calculated Cp_2MCl_2 and Cp_2MO molecular geometries and D(M═O) values at the MP2 level are in favorable agreement with experiment. The D(M═O) and D(M−O) data provide significant insight into the chemistry of Cp_2MO complexes, especially in regard to constraints on oxo transfer as well as oxametallacycle formation and scission processes.

Transition metal oxo complexes play pivotal roles in numerous important biological and abiological stoichiometric and catalytic processes by which oxo functionalities are transferred to organic substrates.[1,2] Despite the importance of such processes and the large synthetic, structural, and mechanistic knowledge base that has been acquired, surprisingly little is known about the energetics of the M≡O/M═O/M−O bonds that are made and broken in such transformations.[1c,3] In the organometallic sphere, groups 4−6 metallocene oxo complexes (**A**) exhibit a particularly rich and diverse chemistry involving a wide variety of transformations of the oxo ligand, including unusual nucleophilic and cycloaddition reaction patterns.[1g,4−6] Many of these transformations raise intriguing, unanswered questions about the strength of the metallocene M═O bonding and the accompanying electronic structures.

A 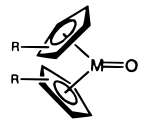

Group 6 metallocene oxo complexes archetypically illustrate many of the complexities and poorly understood features of this class of compounds. Although the M = Mo and W complexes are isolable and display elaborate, interesting chemistries, efficient synthetic routes to the chemically interconnected $Cp_2MH_2 \rightarrow Cp_2MX_2 \rightarrow Cp_2MO$ series have been conspicuously elusive, with a substantial literature chronicalling the difficulties. In regard to molecular and electronic structure, the origins of the curious elongation of Mo−C(Cp) distances on proceeding from Cp_2MoX_2 to Cp_2MoO,[6h] the elongation of the Mo−O distance versus what might be expected,[6h] and the apparent nucleophilicity of the oxo group[6b,c] are not well-understood. While earlier electronic structure studies at the extended Hückel[7a] and Xα-SW[6g] levels focused on providing a *qualitative* understanding of photoelectron and optical spectroscopic fea-

[†] Northwestern University.
[‡] Università della Basilicata.
[⊥] Università di Catania.

(1) (a) Enemark, J. H.; Young, C. G. *Adv. Inorg. Chem.* **1993**, *40*, 1−88. (b) Woo, L. K. *Chem. Rev.* **1993**, *93*, 1125−1136. (c) Holm, R. H.; Donahue, J. P. *Polyhedron* **1993**, *12*, 571−589. (d) Que, L. J. In *Bioinorganic Catalysis*; Reedijk, J., Ed.; Marcel Dekker: New York, 1993; pp 347−393. (e) Holm, R. H. *Coord. Chem. Rev.* **1990**, *100*, 183−221. (f) Nugent, W. A.; Mayer, J. M. *Metal−Ligand Multiple Bonds*; Wiley: New York, 1988. (g) Bottomley, F.; Sutin, L. *Adv. Organomet. Chem.* **1988**, *28*, 339−396. (h) Holm, R. H. *Chem. Rev.* **1987**, *87*, 1401−1449.

(2) (a) Sharpless, K. B. *Tetrahedron* **1994**, *50*, 4235−4258 and references therein. (b) Jacobsen, E. N.; Deng, L.; Furukawa, Y.; Martinez, L. *Tetrahedron* **1994**, *50*, 4323−4334 and references therein.

(3) (a) Conry, R. R.; Mayer, J. M. *Inorg. Chem.* **1990**, *29*, 4862−4867. (b) Watt, G. D.; McDonald, J. W.; Newton, W. E. *J. Less-Common Met.* **1977**, *54*, 415−423.

(4) Group 4: (a) Lee, S. Y.; Bergman, R. G. *J. Am. Chem. Soc.* **1996**, *118*, 6393−6406. (b) Schwartz, D. J.; Smith, M. R., III; Andersen, R. A. *Organometallics* **1996**, *15*, 1446−1450. (c) Polse, I. L.; Andersen, R. A.; Bergman, R. G. *J. Am. Chem. Soc.* **1995**, *117*, 5393−5394. (d) Howard, W. A.; Parkin, G. *J. Am. Chem. Soc.* **1994**, *116*, 606−615. (e) Carney, M. J.; Walsh, P. J.; Hollander, F. J.; Bergman, R. G. *Organometallics* **1992**, *11*, 761−777. (f) Howard, W. A.; Waters, M.; Parkin, G. *J. Am. Chem. Soc.* **1993**, *115*, 4917−4918. (g) Smith, M. R., III; Matsunaga, P. T.; Andersen, R. A. *J. Am. Chem. Soc.* **1993**, *115*, 7049−7050.

(5) Group 5: ref 4e.

S0002-7863(97)01010-X CCC: $15.00 © 1998 American Chemical Society
Published on Web 03/25/1998

tures, respectively, these formalisms are by their nature inherently limited.[7b,c] *Quantitative* descriptions of molecular properties such as geometric structure, bonding energetics, and electronic ground state necessarily require sophisticated approaches which include large basis sets and appropriate treatment of electron correlation.

In the present contribution, we report a combined synthetic, molecular structure, and solution reaction thermochemical study of bonding and bonding energetics in the $(MeCp)_2MO$ series (**A**, M = Mo, W). This includes efficient, high-yield synthetic routes to the $(MeCp)_2MH_2/Cp_2MH_2$, $(MeCp)_2MCl_2/Cp_2MCl_2$, and $(MeCp)_2MoO/Cp_2MO$ series, the crystal structure of $(MeCp)_2WO$ (to allow comparison to trends in the Mo series), and a reaction calorimetric study of interconnected bonding energetics in the $Cp_2MX_2/Cp_2MO/Cp_2M(X)OSiR_3$ series. Combined with detailed ab initio Hartree−Fock and Moller−Plesset level calculations on all members of the group 6 $Cp_2MCl_2/Cp_2MO/Cp_2M(Cl)OSiH_3$ series, these results provide a deeper understanding of metallocene oxo complex electronic structure, molecular geometry, bond strengths, and chemical reaction patterns.[8]

Experimental Section

Materials and Methods. All manipulations of organometallic complexes were carried out under an atmosphere of purified argon using standard high-vacuum techniques, or in a Vacuum Atmospheres glovebox under purified nitrogen (<1 ppm of O_2). Solvents used were predried from appropriate drying agents. The 1,2-dimethoxyethane (DME) used in the calorimetric measurements was additionally stored over Na/K alloy and vacuum transferred into flame-dried glassware immediately prior to use. Me_3SiCl (TMSCl) and Me_3SiI (TMSI) (Aldrich) were purified as described below. ^{1}H NMR spectra were recorded on a Varian XL-400 (400 MHz) or Gemini (300 MHz) spectrometer. Infrared spectra were recorded on Nujol mulls (prepared in the glovebox) using a Mattsen FTIR spectrometer. Elemental analyses were performed by Oneida Research Services, Whitesboro, NY.

A. Metallocene Oxo Complex Syntheses. $(MeCp)_2Mo$═O. 1. Synthesis of $(MeCp)_2MoH_2$. A 250 mL Schlenk flask with magnetic stirring bar was connected to a 100 mL pressure-equalizing addition funnel having a rubber septum as the stopper (see the Supporting Information for a diagram of the apparatus). In the glovebox, the flask was charged with 9.30 g (108 mmol) of Li(MeCp) and 1.8 g (47 mmol) of $NaBH_4$, and the addition funnel charged with 5.0 g (18 mmol) of $MoCl_5$ (Aldrich, 98%). The apparatus was then removed from the glovebox and attached to the Schlenk line. Then, 150 mL of THF was added to the reaction flask via syringe, and a cannula having a nitrogen flow was inserted through the septum of the addition funnel to aid dissolution of the $MoCl_5$ and to prevent clogging of the funnel stopcock. Then, via syringe, 5 mL of −78 °C dry pentane was added to the addition funnel to cover the metal chloride. While the cannula N_2 flow was increased to induce vigorous agitation, 30 mL of −78 °C THF was slowly added via cannula to the addition funnel to dissolve the $MoCl_5$. Next, the resulting $MoCl_5$ solution was added dropwise to the vigorously stirred, 0 °C Li(MeCp) + $NaBH_4$ suspension. The mixture was then allowed to warm to room temperature and finally brought to reflux for 2 h. The solvent was next removed under vacuum, the $(MeCp)_2MoH_2$ extracted with 100 mL of pentane (toluene for the Cp_2Mo analogue), and the mixture filtered. Removal of the solvent from the filtrate in vacuo afforded the yellow-brown product (∼90% yield) which can be used immediately for preparation of $(MeCp)_2MoCl_2$. If purer $(MeCp)_2MoH_2$ is required, the crude material obtained prior to pentane extraction can be sublimed at ∼80 °C, 10^{-4} Torr, affording a 51% yield (based on $MoCl_5$).

2. Synthesis of $(MeCp)_2MoCl_2$. The crude product from step 1 was transferred to a reaction frit assembly and the assembly attached to the high-vacuum line. Next, 60 mL of $CHCl_3$ was vacuum transferred onto the $(MeCp)_2MoH_2$, and the resulting mixture stirred overnight. Solvent was then removed under vacuum, affording a dark green solid. This crude product can be used immediately for the preparation of $(MeCp)_2Mo$═O. If purer $(MeCp)_2MoCl_2$ is required, the solid residue is redissolved in THF and filtered. The solvent is then removed under vacuum and the residue washed with 3 × 5 mL of toluene and 10 mL of pentane, affording a ∼85% yield, based on $MoCl_5$. Pure crystalline material can also be obtained by pentane diffusion into a CH_2Cl_2 solution, followed by slow cooling to −78 °C.

3. Synthesis of $(MeCp)_2Mo$═O. In air, 1.0 g (3.0 mmol) of $(MeCp)_2MoCl_2$ and 3.0 g (75 mmol) of NaOH were quickly weighed into a reaction frit assembly. The assembly was then attached to the high-vacuum line, evacuated, and back-filled 3× with argon. Next, 10 mL of THF and 20 mL of degassed water were added via vacuum transfer and syringe, respectively. The assembly was wrapped with Al foil to exclude light, the solution stirred for 2 h, and the solvent volume then reduced by ∼2/3 under vacuum (removing most THF and some water) to yield a green precipitate. More product precipitation was induced by cooling to 2−4 °C, and the bright green product was collected by filtration and dried under high vacuum. The crude solid was then dissolved in toluene to yield a saturated solution and filtered, and the filtrate slowly cooled to −40 °C. Cold filtration and washing with pentane afforded 0.72 g (89% yield) of bright green crystals. ^{1}H NMR (300 MHz, 25 °C, C_6D_6): δ 1.68 (s, 6H, Me), 4.21("t", J = 2.0 Hz, 4H, CpH), 5.91 ("t", J = 2.0 Hz, 4H, CpH), in agreement with the literature.[6h]

$(MeCp)_2W$═O. 1. Synthesis of $(MeCp)_2WH_2$. The procedure outlined above for $(MeCp)_2MoH_2$ was followed with 6.50 g (75.6 mmol) of Li(MeCp), 1.3 g (33 mmol) of $NaBH_4$, and 5.0 g (12.6 mmol) of WCl_6 (Aldrich, 98%). Similar workup yielded the crude product (4.3 g) as a bright yellow solid in 93% yield. This product can be used immediately for preparation of the corresponding dichloride. If purer $(MeCp)_2WH_2$ is required, the crude product can be sublimed at ∼80 °C, 10^{-4} Torr, affording a ∼60% yield (based on WCl_6). ^{1}H NMR (300 MHz, 25 °C, C_6D_6): δ −11.38 (s + d, 2H, H−W; $J^{123}_{W-^1H}$ = 57 Hz); 2.09 (s, 6H, Me); 4.01 (t, 4H, CpH); 4.40 (t, 4H, CpH).

2. Synthesis of $(MeCp)_2WCl_2$. The procedure outlined above for $(MeCp)_2MoCl_2$ was followed with the crude $(MeCp)_2WH_2$ prepared above. Similar workup yielded a dark green product which can be used immediately in the synthesis of $(MeCp)_2W$═O. If purer $(MeCp)_2WCl_2$ is required, the solid residue is redissolved in THF and filtered through a frit. The solvent is removed under vacuum, and the residue is washed with 3 × 5 mL of toluene and then with 10 mL of pentane, affording an 85% yield (based on WCl_6). Pure crystalline material can be obtained by pentane diffusion into a CH_2Cl_2 solution, followed by slow cooling to −78 °C. ^{1}H NMR (300 MHz, 25 °C, C_6D_6): δ 1.89 (s, 6H, Me); 4.39 ("t", 4H, CpH); 4.49 ("t", 4H, CpH).

3. Synthesis of $(MeCp)_2W$═O. In air, 2.0 g (4.8 mmol) of $(MeCp)_2WCl_2$ and 6.0 g (150 mmol) of NaOH were charged into a high-vacuum frit assembly fitted with two 100 mL flasks. The assembly was attached to the high-vacuum line, evacuated, and back-filled 3× with argon. Next, 10 mL of THF and 20 mL of degassed water were added via vacuum transfer and syringe, respectively. The assembly was then wrapped with Al foil to exclude light, and the solution stirred

(6) Group 6: (a) Henary, M.; Kaska, W. C.; Zink, J. I. *Inorg. Chem.* **1991**, *30*, 1674−1676. (b) Pilato, R. S.; Housmekerides, C. E.; Jernakoff, P.; Rubin, D.; Geoffroy, G. L.; Rheingold, A. L. *Organometallics* **1990**, *9*, 2333−2341. (c) Pilato, R. S.; Rubin, D.; Geoffroy, G. L.; Rheingold, A. L. *Inorg. Chem.* **1990**, *29*, 1986−1990. (d) Parkin, G.; Bercaw, J. E. *J. Am. Chem. Soc.* **1989**, *111*, 391−393. (e) Parkin, G.; Bercaw, J. E. *Polyhedron* **1988**, *1*, 2053−2082. (f) Parkin, G.; Marsh, R. E.; Schaefer, W. P.; Bercaw, J. E. *Inorg. Chem.* **1988**, *27*, 3262−3264. (g) Silavwe, N. D.; Bruce, M. R. M.; Philbin, C. E.; Tyler, D. R. *Inorg. Chem.* **1988**, *27*, 4669−4676. (h) Silavwe, N. D.; Chiang, M. Y.; Tyler, D. R. *Inorg. Chem.* **1985**, *24*, 4219−4221. (i) Berry, M.; Davies, S. G.; Green, M. L. H. *J. Chem. Soc., Chem. Commun.* **1978**, 99−100. (j) Green, M. L. H.; Lynch, A. H.; Swanwick, M. G. *J. Chem. Soc., Dalton Trans.* **1972**, 1445−1447.

(7) (a) Bridgman, A. J.; Davis, L.; Dixon, S. J.; Green, J. C.; Wright, I. N. *J. Chem. Soc., Dalton Trans.* **1995**, 1023−1027 (EHMO and PES studies of $(MeCp)_2MoO$ and $(MeCp)_2WO$). For a discussion of the limitations of these computational techniques, see: (b) Lipkowitz, K. B.; Boyd, D. B. *Computational Chemistry*; VCH: New York, 1994. (c) Russo, T. V.; Martin, R. L.; Hay, P. J. *J. Chem. Phys.* **1994**, *101*, 7729−7737.

(8) Communicated in part: Luo, L.; Di Bella, S.; Lanza, G.; Fragalà, I.; Stern, C. L.; Marks, T. J. *Abstracts of Papers*, 212th National Meeting of the American Society, Orlando, FL., August 25−29, 1996; American Chemical Society: Washington, DC, 1996; INOR 358.

for 2 h. Next, the volume of the solvent mixture was reduced by ∼2/3 in vacuo to yield a dark green (sometimes purple-blue) precipitate. More product precipitated on cooling to near 0 °C. The dark green (sometimes purple-blue) solid material was then collected by filtration and dried under high vacuum. The solid was dissolved in toluene to afford a saturated solution and filtered, and the filtrate slowly cooled to −40 °C. Cold filtration and washing with pentane afforded 1.4 g (82% yield) of dark green crystals. ^{1}H NMR (300 MHz, 25 °C, C_6D_6): δ 1.68 (s, 6H, Me); 4.21 ("t", J = 2.3 Hz, 4H, CpH); 5.91 ("t", J = 2.2 Hz, 4H, CpH). FTIR (Nujol mull, NaCl plates, cm^{-1}): 850 (vs), ν(W═O). Anal. Calcd for $WOC_{12}H_{14}$: C, 40.25; H, 3.94; Found: C, 40.20; H, 4.16.

B. ^{1}H NMR Titrations for Calorimetric Reactions. Reactions for calorimetry were investigated via ^{1}H NMR titrations to ascertain if each was quantitative and sufficiently rapid for accurate thermochemical measurements. In a Wilmad screw-capped NMR tube fitted with a septum, a known amount of complex was dissolved in C_6D_6 and reacted with a solution of the calorimetry reagent, TMSCl or TMSI, in C_6D_6 by incremental injection using a Hamilton gas-tight syringe. Each injection was followed by vigorous shaking and NMR spectral analysis. Only rapid and complete reactions were used in titration calorimetry.

C. Titration Calorimetry. Solution titration calorimetry was performed with a Tronac Model 450 isoperibol calorimeter extensively modified for extremely air- and moisture-sensitive compounds.[9] The instrument was calibrated using the reaction of $(HOCH_2)_3CNH_2$ with HCl in water. The derived enthalpies for this standard reaction compared closely to literature values.[10] Only materials of high purity as indicated by IR and NMR spectroscopies and elemental analysis were used in calorimetric experiments. The heats of solution of $(MeCp)_2MoO$, $(MeCp)_2WCl_2$, and $(MeCp)_2WO$ in toluene were measured by breaking ampules of the complexes of interest in the toluene-filled calorimeter reaction dewar. The derived heats of solution at 25.00(1) °C are 3.2(2), 2.9(1), and 3.3(4) kcal/mol, respectively.

1. Calorimetric Titration of $(MeCp)_2Mo$═O with Me_3SiCl in DME. Fresh TMSCl was refluxed over activated Davison 4A molecular sieves, vacuum transferred into a flask containing P_2O_5, and stirred overnight. Then, on the high-vacuum line, approximately 2 mL of TMSCl was vacuum transferred into a 100 mL volumetric flask fitted with a J-Young valve which could be connected to the calorimeter. This transfer was followed by vacuum transferring sufficient dry DME to fill the volumetric flask. The flask was then connected to the calorimeter. In the glovebox, freshly prepared $(MeCp)_2Mo$═O was carefully weighed (100−200 mg) into an Al foil-wrapped 5.00 mL volumetric flask having a J-Young valve which could be connected to the calorimeter titrant syringe. The flask was removed from the glovebox and attached to the high-vacuum line. Slightly less than 5.00 mL of DME was vacuum transferred into the flask. The flask was then filled exactly to the 5.00 mL mark with DME using a dry, degassed syringe, and was then connected to the calorimeter. The calorimeter system was evacuated and back-filled with argon three times. Next, both the TMSCl solution and the oxo complex standard solution were introduced into the reaction dewar and the Al foil-wrapped titrant syringe, respectively, under vacuum. The system was then placed under an Ar atmosphere, stirring was initiated, and both the reaction dewar and titrant syringe were lowered into the constant-temperature bath of the apparatus (25.000 ± 0.001 °C) for thermal equilibration. A series of electrical calibration runs was performed before, during, and after titration. A series of metal oxo complex solution injections was then carried out using the calibrated motor-driven buret (ca. 8−12 individual injections per run). An experimental heat capacity was then derived from the electrical calibration runs. Given the molarity of the titrant and the buret delivery rate, the enthalpy of reaction could be calculated. The above procedure was repeated three times, and the resulting average ΔH^{rxn} and standard deviation are reported in Table 3.

2. Calorimetric Titration of $(MeCp)_2W$═O with Me_3SiI in DME. In the glovebox, a freshly prepared $(MeCp)_2W$═O sample was carefully weighed (200−300 mg) into an Al foil-wrapped 5.00 mL volumetric flask having a J-Young valve which could be connected to the calorimeter titrant syringe. A DME solution of $(MeCp)_2W$═O was prepared as described above, and the solution was introduced into the foil-wrapped titrant syringe. Due to the low thermal/photochemical stability of TMSI, instead of introducing a TMSI DME solution into the reaction dewar, approximately 5 mL of fresh TMSI, stabilized with copper chips, was immediately vacuum transferred into the cold (−78 °C) reaction dewar which also contained copper chips. Approximately 95 mL of DME was vacuum transferred into a 100 mL volumetric flask fitted with a J-Young valve which could be connected to the reaction dewar. The volumetric flask containing DME was kept in a dry ice-acetone bath and connected to the reaction dewar. The system was then evacuated and back-filled with Ar three times. While the volumetric flask was still cold, the solvent was introduced into the reaction dewar, the system was placed under an Ar atmosphere, stirring was initiated, and the reaction dewar was maintained at −78 °C overnight. The reaction dewar was then allowed to warm to room temperature. Next, 1.0 mL of standard metal oxo complex solution in the titrant syringe was added to the TMSI solution to destroy any possible reactive impurities. Only colorless solutions (no I_2 produced via the decomposition of TMSI) were used for the subsequent titrations. The system was then lowered into the constant-temperature bath of the apparatus (25.000 ± 0.001 °C) for thermal equilibration. Thermal equilibration was minimized to the shortest possible period. A series of metal oxo complex solution injections was next carried out using the calibrated motor-driven buret (ca. 6−7 individual injections per run). A series of electrical calibration runs was then performed after the titration, and an experimental heat capacity was derived from the electrical calibration runs. Given the molarity of the titrant and the buret delivery rate, the enthalpy of reaction could be calculated. The above procedure was repeated in triplicate, and the resulting average ΔH^{rxn} and standard deviation are reported in Table 3.

3. Calorimetric Titration of $(MeCp)_2W$═O with Me_3SiCl in Toluene. This procedure was the same as for experiment 1 above except that a toluene solution of $(MeCp)_2W$═O was used as the standard solution and TMSCl in toluene as the bulk solution.

4. Calorimetric Titration of $(MeCp)_2Mo$═O with Me_3SiI in DME. This procedure was the same as for experiment 2 above except that a DME solution of $(MeCp)_2Mo$═O was used as the standard solution. The derived ΔH^{rxn} and standard deviation from three determinations are reported in Table 4.

D. X-ray Crystallographic Study of $(MeCp)_2W$═O. After the removal of water and THF in synthetic step 3 above, toluene was added with warming (40−45 °C) to the residue to yield a saturated solution. The solution was then filtered, with gentle heating with a heat gun used to warm the filter frit walls to avoid crystallization. The deep blue (sometimes purple) solution was then allowed to stand at room temperature overnight in the dark. The solution was then placed in an acetone bath, followed by slow cooling with dry ice−acetone (−5 °C/10 min) to −78 °C. Cold filtration afforded dark green crystals suitable for single-crystal diffraction analysis. The crystals were mounted on glass fibers and transferred to the cold N_2 stream (−120 °C) of the Enraf-Nonius CAD4 diffractometer. Final cell dimensions were obtained by least-squares fits to the automatically centered settings for 25 reflections. Three reference reflections monitored during data collection for each crystal showed no significant variations. Intensity data were all corrected for absorption, anomalous dispersion, Lorentz, and polarization effects.[11] The space group choice for the complex was unambiguously determined. Unit cell and data collection parameters are summarized in Table 1.

Subsequent computations were carried out on a micro Vax 3600 computer. The structure was solved by direct methods (SHELXS-86).[12] The non-hydrogen atoms were refined anisotropically. Hydrogen atoms

(9) (a) King, W. A.; Di Bella, S.; Lanza, G.; Khan, K.; Duncalf, D. J.; Cloke, F. G. N.; Fragala, I. L.; Marks, T. J. *J. Am. Chem. Soc.*, **1996**, *118*, 627−635. (b) King, W. A.; Marks, T. J. *Inorg. Chim. Acta* **1995**, *229*, 343−354. (c) Nolan, S. P.; Stern, D.; Marks, T. J. *J. Am. Chem. Soc.* **1989**, *111*, 7844−7854. (d) Schock, L. E.; Marks, T. J. *J. Am. Chem. Soc.* **1988**, *110*, 7701−7715.

(10) Eatough, D. J.; Christensen, J. J.; Izatt, R. M. *Experiments in Thermometric Titrimetry and Titration Calorimetry*; Brigham Young University Press: Provo, UT, 1974; pp 49−51.

(11) Cromer, D. T.; Waber, J. T. *International Tables for X-ray Crystallography*; The Kynoch Press: Birmingham, England, 1974; Vol. IV, pp 149−150.

Table 1. Crystal Data and Structural Analysis Results for $(CpMe)_2W{=}O$

empirical formula	$WC_{12}H_{14}O$
crystal dimensions (mm)	$0.32 \times 0.27 \times 0.06$
space group	$P2_12_12_1$ (no. 19)
unit cell dimensions	
a, Å	6.687(2)
b, Å	9.282(2)
c, Å	16.427(4)
V, Å^3	1019.6(4)
Z, molecules/cell	4
density(calcd), g/cm^3	2.333
temperature, °C	−120.0
X-ray wavelength, Å	Mo Kα, 0.710 69
diffractometer	Enraf-Nonius CAD4
monochromator	highly ordered graphite crystal
scan type	$\omega-\theta$
2θ range, deg	25 (21.9−25.7)
no. of obsd reflns ($I > 3\sigma$)	1240
reflection/parameter ratio	9.69
residuals: R; R_w	0.019; 0.025
goodness of fit	2.2
number of parameters	821

were fixed in idealized positions. The maximum peak on the final difference Fourier map (1.02 e Å^{-3}) was located in the vicinity of the W positions. Neutral atom scattering factors were taken from Cromer and Waber.[13] Anomalous dispersion effects were included in Fcalc,[14] and the values for $\Delta f'$ and $\Delta f''$ were those of Creagh and McAuley.[15] The values for the mass attenuation coefficients were those of Creagh and Hubbel.[16] All calculations were performed using the TEXSAN[17] crystallographic software package of Molecular Structure Corp.

Computational Details

The relativistic effective core potentials (RECPs) developed by Stevens et al.[18] were used for the silicon and chlorine atoms to enhance computational efficiency. For transition metals, the RECPs explicitly treat the subvalence $(n-1)s^2$ and $(n-1)p^6$ electrons. The standard 6-31G basis sets of Pople et al. were adopted for the C, O, and H atoms.[19] The geometries of all states presently analyzed were fully optimized, using gradient techniques at the Hartree−Fock level. More accurate values of relative stabilities of possible, different electronic states and, in turn, of the bond dissociation enthalpies were evaluated using single point MP2, MP3 and MP4(SDQ) energy calculations on the optimized HF geometries. The influence of correlation effects on geometrical structures and dissociation energies was fully evaluated through MP2 geometry optimization of Cp_2WO and Cp_2W. In the MPn procedure, all of the valence electrons (except the 1s core electrons of C and O atoms) are correlated. Thermodynamic data were evaluated, at various levels of theory, adopting simple model reactions: (eqs 1, 2). Here, all models have unsubstituted Cp rings and a simpler H_3Si-

$$\text{M=O BDE:}\quad Cp_2M{=}O \rightarrow Cp_2M + O \qquad (1)$$

$$\text{M−O BDE:}\quad Cp_2M{=}O + H_3SiCl \rightarrow Cp_2MCl(OSiH_3) \qquad (2)$$

group on the silyl chloride reagent. Nevertheless, these approximations are expected to introduce no greater than a few kilocalories per mole variation in the calculated bond enthalpy values.[9a] Calculations on the required product molecules Cp_2M and $Cp_2MCl(OSiH_3)$ were performed at the same level of theory. In particular, the energies of the possible $^3A_{2g}$ (e_{2g}^2, a_{1g}^2) and $^3E_{2g}$ (e_{2g}^3, a_{1g}^1) low-lying states of the open-shell, d^4 Cp_2M (M = Cr, Mo, W) complexes were evaluated. In all cases, the $^3E_{2g}$ state was found to be lowest in energy, in agreement with experimental results.[20] Metrical parameters associated with the $^3E_{2g}$ state of Cp_2Cr are in good agreement with those determined by gas-phase electron diffraction.[21] Calculations on $Cp_2MCl(OSiH_3)$ complexes were carried out without any symmetry constraints. Validation of the predicted geometries is hampered by the lack of experimental structural data even though the present Mo−O bond length (1.981 Å) is close to that reported for $[Cp_2Mo(OH)NH_2CH_3]^+PF_6^-$ (2.05 Å).[22] All the calculations were performed using the HONDO-95.3[23] and Gaussian-94[24] programs on IBM SP and Cray C92 systems.

Results

This section begins with a discussion of improved synthetic routes to group 6 $Cp_2MH_2/Cp_2MCl_2/Cp_2Mo$-type complexes and molecular structural information, followed by an account of the reaction chemistry employed to measure heats of reaction and to derive metal−oxo and metal−alkoxide bond enthalpies. Next, computational results are presented, focusing on derived molecular structures, electronic structure, bonding patterns, and calculated bonding energetics. Finally, known and prospective Cp_2MO reaction patterns are analyzed in light of the derived M=O/M−O bond enthalpies.

Synthesis of Cp_2MO Complexes. The traditional approach to $Cp_2M{=}O$ complexes (M = Mo, W) involves treating the corresponding Cp_2MCl_2 complexes with aqueous KOH or NaOH solution. The Cp_2MCl_2 precursor can in turn be obtained from reaction of Cp_2MH_2 with $CHCl_3$. However, reproducible, high-yield syntheses of Cp_2MH_2 complexes have long been elusive.[25] Frequently, intractable oily material is obtained which is difficult to dry, and little dihydride can be recovered by sublimation. This problem is even more acute for Cp_2WH_2. Furthermore, even when metallocene oxo complexes are obtained by these routes, purification is still difficult and has hindered detailed study of these complexes.[25]

Considerable effort has been expended in developing reproducible, high-yield syntheses of $Cp_2M{=}O$ complexes. An improved Cp_2MoH_2 procedure involves treatment of $MoCl_5$ with NaCp and $NaBH_4$ in THF−hexane, with yields of ∼40% attainable in 5−6 days.[25b] A 4-day preparation of Cp_2WH_2 from WCl_6 and NaCp + $NaBH_4$ has also been reported.[25c] In the latter, a laborious procedure which includes $HCl_{(aq)}$ extraction,

(12) Sheldrick, G. M. In *Crystallographic Computation*; Sheldrick, G. M., Kruger, C., Goddard, R., Eds.; Oxford University Press: Oxford, 1985; pp 175−189.
(13) Reference 26, Vol. IV, Table 2.2A.
(14) Ibers, J. A.; Hamilton, W. C. *Acta Crystallogr.* **1964**, *17*, 781−782.
(15) Creagh, D. C.; McAuley, W. J. In *International Tables for Crystallography*; Wilson, A. J. C., Ed.; Kluwer Academic Publishers: Boston, 1992; Vol. C, Table 4.2.6.8, pp 219−222.
(16) Creagh, D. C.; Hubbel, J. H. In *International Tables for Crystallography*; Wilson, A. J. C., Ed.; Kluwer Academic Publishers: Boston, 1992; Vol. C, Table 4.2.4.3, pp 200−206.
(17) *TEXSAN Structure Solution Package*; Molecular Structure Corp.: The Woodlands, TX, 1985 and 1992.
(18) (a) Stevens, W. J.; Krauss, M.; Basch, H.; Jansien, P. G. *Can. J. Chem.* **1992**, *70*, 612−630. (b) Stevens, W. J.; Basch, H.; Krauss, M. *J. Chem. Phys.* **1984**, *81*, 6026−6033.
(19) Hehre, W. J.; Radom, L.; Schleyer, P. V. R.; Pople, J. A. *Ab Initio Molecular Orbital Theory*; Wiley: New York, 1986.
(20) (a) Cox, P. A.; Grebenik, P.; Perutz, R. N.; Robinson, M. D.; Grinter, R.; Stern, D. *Inorg. Chem.* **1983**, *22*, 3614−3620. (b) Chotwynd-Talbot, J.; Grebenik, P.; Perutz, D. *Inorg. Chem.* **1982**, *21*, 3647−3657.
(21) Gard, E.; Haaland, A.; Novak, D. P.; Seip, R. *J. Organomet. Chem.* **1975**, *88*, 181−184.
(22) Prout, K.; Cameron, T. S.; Forder, R. A.; Critchiley, S. R.; Denton, B.; Rees, G. V. *Acta Crystallogr.* **1974**, *B30*, 2290−2304.
(23) Dupuis, M.; Marquez, A.; Davidson, E. R. *HONDO 95.3 from CHEM-Station*; IBM Corp.: Kingston, NY, 1995.
(24) Frisch, M. J.; Trucks, G. W.; Schlegel, H. B.; Gill, P. M. W.; Johnson, B. J.; Robb, M. A.; Cheeseman, J. R.; Keith, T. A.; Petersson, G. A.; Montgomery, J. A.; Raghavachari, K. Al-Laham, M. A.; Zakrzewski, V. G.; Ortiz, J. R.; Foresman, J. B.; Head-Gordon, M.; Wong, M. W.; Replogle, E. S.; Gomperts, R.; Andres, J. L.; Binkley, J. S.; Gonzalez, C.; Martin, R. L.; Fox, D. J.; Degrees, D. J.; Baker, J.; Steward, J. J. P.; Pople, R.; *Gaussian-94*; Gaussian Inc.: Pittsburgh, PA, 1995.
(25) (a) Green, M. L. H.; McCleverty, J. A.; Pratt, L.; Wilkinson, G. *J. Chem. Soc.* **1961**, 4854−4859. (b) Silavwe, N. D.; Castellani, M. P.; Tyler, D. R. In *Inorganic Synthesis;* Grimes, R. N., Ed.; John Wiley and Sons: New York, 1992; Vol. 29, pp 204−211. (c) Green, M. L. H.; Knowles, P. J. *J. Chem. Soc., Perkin Trans. 1* **1973**, 989−991. (d) Bashkin, J.; Green, M. L. H.; Poveda, M. L.; Prout, K. *J. Chem. Soc., Dalton Trans.* **1982**, 2485−2494. (e) Andersson, C.; Persson, C. *Organometallics* **1993**, *12*, 2370−2373.

filtration through silica gel and alumina, sublimation, etc. is necessary to obtain a 46% yield. A second procedure involving reaction of $Mo_2(O_2CCH_3)_4$, NaCp, and PPh_3, followed by the addition of $HCl_{(aq)}$, was also reported for Cp_2MoCl_2.[25d] Although it provides the dichloride in higher overall yield, it is not readily adapted to complexes with substituted Cp ligands.[26] More recently, an improved preparation of WCl_4(DME) allowed the synthesis of Cp_2WH_2 in 42% yield by reaction with LiCp and $LiAlH_4$.[25e]

To prepare pure Cp_2MO and Cp_2WO for calorimetry and structural characterization, we investigated why insoluble, oily products form in the original synthetic procedure,[25a] which offers the simplest methodology from commercially available reagents. An initial conjecture was that high local temperatures develop at the metal chloride surface because of the highly exothermic reaction, exacerbated by the difficulty of effecting slow addition of a solid reagent. The observed evolution of yellow-green smoke suggests high local temperatures, which may produce thermolytic byproducts. Furthermore, the oily byproduct coats the metal chloride surface, forming lumpy material which hinders further reaction, thus degrading the yield. Taking advantage of $MoCl_5$ and WCl_6 solubility in THF, the metal chloride was first dissolved in cold (−78 °C) THF, and the resulting solution added dropwise to the rapidly stirring THF suspension of LiCp and $NaBH_4$. Smoke was not observed, and the reaction was not significantly exothermic. The generation of byproducts could thus be controlled, and yields were significantly increased. Furthermore, while no lumpy material forms, the resulting product is still difficult to dry. Noting a report that refluxing NaCp or LiCp THF solutions with the metal chlorides consumes stoichiometrically excess NaCp or LiCp (presumably in redox-related chemistry),[27] the LiCp:MCl_n (n = 5, M = Mo; n = 6, M = W) molar ratio was increased, and at 6:1 (<4.5:1 is used in other procedures) a dry product is formed. Subsequent sublimation affords the dihydride in higher yield than in any previously reported procedure. Furthermore, the dihydride can be extracted with toluene (for Cp complexes) or hexane (for MeCp complexes) to afford satisfactory product in 90% and 93% yields for Cp'_2MoH_2 and Cp'_2WH_2 (Cp′ = Cp or MeCp), respectively. This procedure is very simple, and the necessity of destroying excess starting material (e.g., with aqueous HCl or NaOH) is eliminated.

The Cp_2MH_2 products resulting from solvent extraction can be immediately converted to the corresponding dichlorides with $CHCl_3$. If purer material is required, the dichloride can be easily recrystallized from pentane/CH_2Cl_2. Due to the photosensitivity of the Mo and W oxo complexes, syntheses are carried out with exclusion of light. The literature procedures require 10 h for aqueous alkaline hydrolysis of the dichlorides;[25b] however, we find reaction is complete in 2−3 h when THF is used as the cosolvent, presumably reflecting increased solubility of the dichlorides. Recrystallization of the products from toluene/pentane affords analytically pure material suitable for calorimetry and single-crystal diffraction analysis. Chromatographic purification is not required. $(MeCp)_2Mo{=}O$ and $(MeCp)_2W{=}O$ can be prepared using similar procedures in the same high yields and purities (see the Experimental Section for details).

(26) Applying this procedure to the preparation of $(MeCp)_2MoCl_2$ was unsuccessful. The yellow-brown solid obtained from refluxing $Mo_2(O_2CCH_3)_4$ with Na(MeCp) and PPh_3 in THF displayed a color different from that (green) of the unsubstituted metallocene dimer. Treatment with HCl afforded negligible $(MeCp)_2MoCl_2$, as indicated by NMR.

(27) Robbins, J. L.; Edelstein, N.; Spencer, B.; Smart, J. C. *J. Am. Chem. Soc.* **1982**, *104*, 1882−1893.

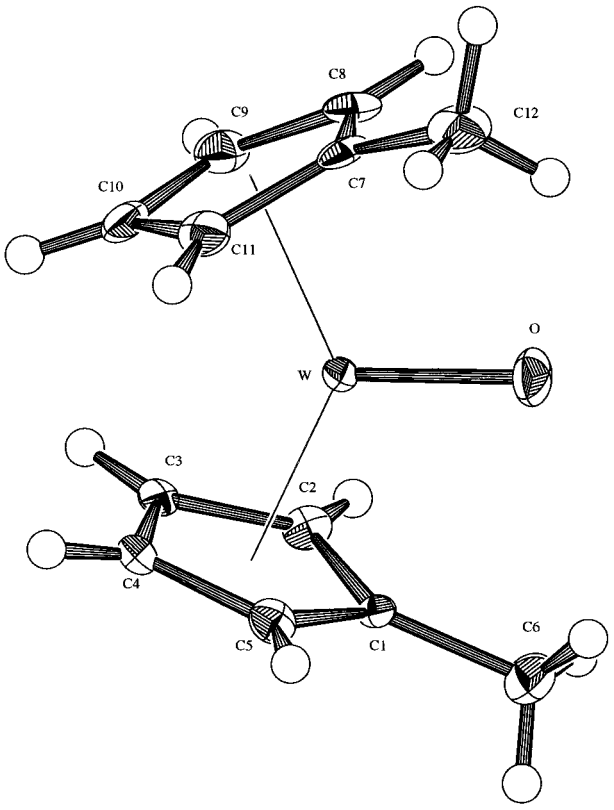

Figure 1. ORTEP drawing of the molecular structure of $(MeCp)_2W{=}O$. All non-hydrogen atoms are represented by thermal ellipsoids drawn to encompass 50% probability, and hydrogen atoms are deleted for ease of viewing.

Table 2. Selected Bond Distances (Å) and Bond Angles (deg) for $(MeCp)_2W{=}O$

Bond Lengths[a]			
W−O	1.744(5)	W−C(1)	2.304(8)
W−C(2)	2.33(1)	W−C(3)	2.446(9)
W−C(4)	2.437(9)	W−C(5)	2.32(1)
W−C(7)	2.411(9)	W−C(8)	2.397(9)
W−C(9)	2.363(10)	W−C(10)	2.376(8)
W−C(11)	2.322(10)	C(1)−C(2)	1.44(1)
C(1)−C(5)	1.44(1)	C(1)−C(6)	1.50(1)
C(2)−C(3)	1.41(1)	C(3)−C(4)	1.42(1)
C(4)−C(5)	1.42(1)	C(7)−C(8)	1.41(1)
C(7)−C(11)	1.44(1)	C(7)−C(12)	1.53(1)
C(8)−C(9)	1.41(1)	C(9)−C(10)	1.44(2)
C(10)−C(11)	1.43(2)	W−Cp_1(cent)	2.03(1)
W−Cp_2(cent)	2.05(1)		
Bond Angles[a]			
O−W−Cp_1(cent)	116.5(6)	W−C(1)−C(6)	120.7(5)
O−W−Cp_2(cent)	111.3(6)	W−C(7)−C(12)	121.3(6)
Cp_1(cent)-W−Cp_2(cent)	132.2(4)		

[a] Numbers in parentheses are the estimated standard deviations.

Molecular Structure of $(MeCp)_2W{=}O$. The molecular structure of $(MeCp)_2W{=}O$ is shown in Figure 1, while selected bond distances and angles are compiled in Table 2. The crystal structure consists of monomeric Cp_2MX units having the classic "bent sandwich" geometry. Although $(MeCp)_2WO$ is formally isostructural with $(MeCp)_2MoO$,[6g] there are significant differences in metrical parameters. The W−O bond length of 1.744(5) Å can be compared with the corresponding Mo−O bond length of 1.721(2) Å, and is thus ∼0.02 Å longer. As noted previously, such distances are somewhat elongated from what might be expected for formal M≡O bonds.[6g,h,7a] The mean M−Cp(cent) distances in $(MeCp)_2Mo{=}O$ and $(MeCp)_2W{=}O$ are essentially identical at 2.05(1) and 2.04(1) Å, respectively. The average M−C distances for these two structures are 2.369-

(3) and 2.371(8) Å, respectively. In the Mo complex, the shortest and longest M−C(Cp) distances are 2.326(4) and 2.419(3) Å, respectively, whereas in the W complex, the corresponding distances are 2.304(8) and 2.446(9) Å, respectively. These metal−ligand bond distance trends are in accord with tabulated trends in six-coordinate Mo^{IV} (0.65 Å) and W^{IV} (0.66 Å) ionic radii.[28] In contrast to much-studied Cp_2MoX_2 complexes,[29] there is a sparse Cp_2WX_2 structural database with which to compare the present results. However the ∼0.07 Å expansion in M−C(Cp) distances in Cp_2MoO vs other Cp_2MoX_2 complexes[29] is also observed for W in proceeding from $[(Me_5Cp)(CO)(NO)Re(\mu_2\text{-}\eta^3\text{-}CO_2)WCp_2]^+BF_4^-$ (2.30 Å)[6b] to $(MeCp)_2WO$ (2.371(8) Å). The present average W−C(Cp) contacts can also be compared to a corresponding distance of 2.37(3) Å in cationic $(Cp_2WCl^+_2)_2W_4F_{18}^{2-}$.[30] The present Cp(cent)−W−Cp(cent) angle of 132.2(4)° is similar to that in $(MeCp)_2MoO$ (133.7°)[6g] and in the above Re, W bimetallic (139.0(9)°).[6b] Interestingly, the present dihedral angle between the staggered Cp−Me groups (expressed as the angle between the W,C(1),C(6) and W,C(7),C(12) planes) is 49°, which is substantially larger than that in $(MeCp)_2MoO$, 29°.[6g]

Thermochemical Measurements and Results. The primary goal of the present thermochemical study was to quantify M═O/M−O bonding energetics with respect to understanding transformations such metallocene oxo complexes undergo. As argued elsewhere,[9,31] solution phase bond enthalpy data are most desirable for analyzing solution phase chemical interconversions, and for nonpolar solvents, should parallel gas-phase trends. Although *absolute* $D(Cp_2M{=}O)$ parameters would be most desirable, the requisite oxo transfer processes (e.g., eq 3 or 4) are not available for this Mo, W series nor are the necessary

$$Cp_2M{=}O + L \rightarrow Cp_2M + L{=}O \quad (3)$$

$$Cp_2M + L{=}O \rightarrow Cp_2M{=}O + L \quad (4)$$

Cp_2M metallocenes stable. However, oxo metathesis processes offer an alternative approach (eq 5) and provide *relative*

$$Cp_2M{=}O + 2YX \rightarrow Cp_2MX_2 + Y_2O \quad (5)$$

$D(Cp_2M{=}O)$ values "anchored" to a substantial existing database of $D(Cp_2M(X)-X)$ parameters.[32] This allows straightforward thermodynamic analysis of numerous Cp_2MO/Cp_2MX_2 interconversion processes. For the present study, it was found that eq 5 can be satisfactorily implemented for YX = trimethylsilyl halides with several provisos. First, the poor solubility of the Cp_2MO/Cp_2MX_2 complexes necessitates the use of $(MeCp)_2MO/(MeCp)_2MX_2$ complexes. Even so, the reaction of $(MeCp)_2MoO$ with TMSCl is slow and stepwise in toluene (eq 6), with complex **B** precipitating. Furthermore, this reaction halts at intermediate **A** in the case of $(MeCp)_2WO$. However,

$$(MeCp)_2Mo{=}O \xrightarrow[\text{toluene}]{\text{TMSCl}} \underset{\mathbf{A}}{(MeCp)_2Mo(OTMS)Cl} \xrightarrow[\text{toluene}]{\text{TMSCl}} \underset{\mathbf{B}}{(MeCp)_2MoCl_2} + TMS_2O \quad (6)$$

the reaction of $(MeCp_2)MoO$ with TMSCl in polar solvents such as DME (THF undergoes ring-opening) is found by ^1H NMR to proceed rapidly and cleanly to **B** (eq 7).

$$(MeCp)_2Mo{=}O \xrightarrow[\text{DME}]{\text{TMSCl}} \underset{\mathbf{B}}{(MeCp)_2MoCl_2} + TMS_2O \quad (7)$$

The reaction of $(MeCp)_2W{=}O$ with TMSCl in DME does not afford $(MeCp)_2WCl_2$ quantitatively, but rather a mixture of the W analogues of **A** and **B** (cf. eq 6). The reaction rate is also significantly slower than for M = Mo. Thus, more reactive TMSI was chosen for thermochemical titrations of $(MeCp)_2W{=}O$ in DME. However, although the reaction to form $(MeCp)_2WI_2$ is rapid and quantitative (eq 8), the instability of the TMSI

$$(MeCp)_2W{=}O \xrightarrow[\text{DME}]{\text{TMSCl}} (MeCp)_2WI_2 + TMS_2O \quad (8)$$

reagent presents an experimental complication. Even under inert atmosphere, TMSI transfer via cannula causes the solution to change from colorless to pale yellow, suggesting I_2 formation. The rate of decomposition can be significantly suppressed by addition of Cu chips as a stabilizer[33] in all TMSI storage and transfer, and by performing all transfers in vacuo in the dark at −78 °C (see the Experimental Section for details). Furthermore, possible reactive impurities in bulk TMSI solutions were destroyed by the addition of the standard solution of $(MeCp)_2WO$ (∼1 mL) prior to calorimetric titrations. This procedure affords reproducible titration results. To verify that the handling of TMSI was appropriate for accurate calorimetry, a second determination of $D((MeCp)_2Mo{=}O)$ was carried out using this reagent rather than TMSCl. It was found that the agreement between the two $D(Mo{=}O)$ measurements is within experimental error (vide infra). Although the reaction of $(MeCp)_2WO$ with TMSCl in toluene was found to halt at intermediate $(MeCp)_2W(OTMS)Cl$, it will be seen that this can be used to derive the W−O single bond enthalpy in $(MeCp)_2W(OTMS)Cl$ since $D(W{=}O)$ is known.

The derivation of $D((MeCp)_2M{=}O)$ values follows from the measured heats of silanolytic metathesis (ΔH^{rxn}) and the thermodynamic cycle of eqs 9−13. Here, $D(Me_3Si-X)$ values

$$Cp_2M{=}O \rightarrow Cp_2M + O \qquad D(M{=}O) \quad (9)$$

$$2Me_3SiX \rightarrow 2Me_3Si^{\bullet} + 2X^{\bullet} \qquad 2D(Me_3Si-X) \quad (10)$$

$$2X^{\bullet} + Cp_2M \rightarrow Cp_2MX_2 \qquad -2\bar{D}(Cp_2M(X)-X) \quad (11)$$

$$2Me_3Si^{\bullet} + O \rightarrow Me_3SiOSiMe_3 \quad -D(Me_3Si-O-SiMe_3) \quad (12)$$

$$Cp_2M{=}O + 2Me_3SiX \rightarrow Cp_2MX_2 + Me_3SiOSiMe_3 \quad \Delta H^{rxn} \quad (13)$$

are taken from the literature,[34] and $D(Me_3Si-O-SiMe_3)$ is

(28) Shannon, R. D. *Acta Crystallogr.* **1976**, *A32*, 751−767.

(29) Kuo, K. Y.; Kanatzidis, M. G.; Sabat, M.; Tipton, A. L.; Marks, T. J. *J. Am. Chem. Soc.* **1991**, *113*, 9027−9045 and references therein.

(30) Camerson, T. S.; Klapötke, T. M.; Schalz, A.; Valkonan, J. *J. Chem. Soc., Dalton Trans.* **1993**, 659−662.

(31) (a) Marks, T. J. In *Bonding Energetics in Organometallic Compounds*; Marks, T. J., Ed.; ACS Symposium Series; American Chemical Society: Washington, DC, 1990; Vol. 428, Chapter 1. (b) Nolan, S. P.; Stern, D.; Hedden, D.; Marks, T. J. In ref 31a, Chapter 12. (c) Nolan, S. P.; Stern, D.; Marks, T. J. *J. Am. Chem. Soc.* **1989**, *111*, 1

(32) (a) Calhorda, M. J.; Carrondo, M. A. A. F.; Dias, A. R.; Gabvao, A. M.; Martins, M. H. G. A. M.; Piedak, M. E. M. D.; Pinheiro, C. I.; Romao, C. C.; Martinho Simoes, J. A.; Veiros, L. F. *Organometallics* **1991**, *10*, 438−483. (b) Martinho Simoes, J. A.; Beauchamp, J. L. *Chem. Rev.* **1990**, *90*, 629−688. (c) Dias, A. R.; Martinho Simoes, J. A. *Polyhedron* **1988**, *7*, 1531−1544.

(33) Olah, G. A.; Narang, S. C. *Tetrahedron* **1982**, *38*, 2225−2277.

(34) (a) Walsh, R. In *The Chemistry of Organic Silicon Compounds*; Patai, S., Rappoport, Z., Eds.; John Wiley & Sons: New York; 1989; Chapter 5, pp 371−391. (b) Walsh, R. *Acc. Chem. Res.* **1981**, *14*, 246−252.

Table 3. Thermochemical Data and Derived M═O Bond Enthalpies

$$(MeCp)_2M{=}O + 2TMSX \xrightarrow[25\ ^\circ C]{DME} (MeCp)_2MX_2 + (TMS)_2O$$

M, X	ΔH^{rxn}	D(M−X)[a] (kcal/mol)	D(Si−O−Si)[b] (kcal/mol)	D(Si−X)[c] (kcal/mol)	D(M═O) (kcal/mol)
Mo, Cl	−62.4(7)	72.7(1.7)	253.0(3.0)	112.9(1.9)	110(11)
Mo, I	−86(2)	49.5(2.1)	253.0(3.0)	76.8(1.9)	112(13)
W, I	−95.2(8)	64.1(1.2)	253.0(3.0)	76.8(1.9)	132(10)

[a] From ref 32b,c. [b] Calculated from ΔH_f values of $Me_3SiOSiMe_3$,[34] Me_3Si,[35] and O.[36] [c] From ref 34a,b.

calculated from tabulated ΔH_f values of $Me_3SiOSiMe_3$,[34] Me_3Si·,[35] and O.[36] The existing literature values for $D(Cp_2M(X)-X)$ were derived from thermochemical data for MCl_6 and heats of combustion of the corresponding metallocene dihalides.[32,37] Although it could be argued that alternative anchor points are better approximations to absolute $D(Cp_2M(X)-X)$ values,[38] we employ the literature Cp_2MX_2 values[32,37] because they represent a broad and internally consistent database. Moreover, these data are in good agreement with absolute $D(CpMo(CO)_3-X)$ values[39] for the same Mo−X bonds. Anchoring to the literature $D(Cp_2M(X)-X)$ data suffices to analyze the great bulk of Cp_2MO/Cp_2MY_2 interconversions (vide infra) and yields $D(Cp_2M{=}O)$ bond enthalpies differing in most cases by less than ∼10−15% from alternative anchor points.[38] As discussed elsewhere[9a] and verified in this study (see the Experimental Section for data), metallocene heats of solution represent a minor contribution to the observed heats of reaction and, for all practical purposes, cancel in eq 13. Thermochemical results are summarized in Table 3, where stated uncertainties represent the *maximum additive* uncertainties derived from the present thermochemical measurements and all tabulated data. Actual uncertainties are likely smaller. The standard deviations reported for ΔH^{rxn} provide an indication of the experimental precision. It can be seen that the D(Mo═O) values are large, with good agreement between parameters derived from TMSCl and TMSI titrations. The value for D(W═O) is considerably larger than that for the Mo analogue.

As noted above, the reaction of $(MeCp)_2WO$ and TMSCl proceeds rapidly and cleanly to the corresponding tungstenocene siloxychloride (eq 14). This transformation was investigated

$$(MeCp)_2W{=}O + TMSCl \rightarrow (MeCp)_2W(OTMS)Cl \quad (14)$$

calorimetrically and the result used to estimate D(W−$OSiMe_3$).

Table 4. Thermochemical Data and Derived W−OTMS Bond Enthalpy

$$(MeCp)_2W{=}O + TMS{-}Cl \xrightarrow[25\ ^\circ C]{Tol} (MeCp)_2W(OTMS)Cl$$

ΔH^{rxn} (kcal/mol)	D(W═O) (kcal/mol)	D(W−Cl)[a] (kcal/mol)	D(Si−O)[b] (kcal/mol)	D(Si−Cl)[c] (kcal/mol)	D(W−O) (kcal/mol)
−38.4(5)	132.4(10.0)	83.1(2)	136.1(4.8)	112.9(1.9)	65(18)

[a] From ref 32b,c. [b] Estimated from $D(Me_3SiO-SiMe_3)$.[41] [c] From ref 34,a,b.

Table 5. Selected HF and MP2 Bond Lengths (Å) and Bond Angles (deg) for Cp_2MO (M = Cr, Mo, W) Complexes.

	$Cp_2Cr{=}O$	$Cp_2Mo{=}O$		$Cp_2W{=}O$	
parameter	calcd	calcd	exptl[a]	calcd[b]	exptl[a]
M−$Cp_{1(cent.)}$	2.010	2.170	2.047	2.153 [2.093]	2.03(1)
M−$Cp_{2(cent.)}$	2.060	2.176	2.044	2.160 [2.115]	2.05(1)
Cp_1−M−Cp_2	138.1	135.1	133.7	132.2 [127.7]	132.2(4)
M−O	1.561	1.719	1.721(2)	1.729 [1.780]	1.744(5)
M−C(1)	2.334	2.459	2.347(3)	2.367 [2.185]	2.304(8)
M−C(2)	2.327	2.457	2.331(4)	2.419 [2.327]	2.33(1)
M−C(3)	2.417	2.518	2.419(3)	2.563 [2.641]	2.446(9)
M−C(4)	2.417	2.518	2.413(3)	2.563 [2.641]	2.437(9)
M−C(5)	2.327	2.457	2.345(3)	2.419 [2.327]	2.32(1)
M−C(7)	2.448	2.521	2.401(3)	2.496 [2.516]	2.411(9)
M−C(8)	2.448	2.521	2.386(3)	2.496 [2.156]	2.397(9)
M−C(9)	2.347	2.464	2.357(4)	2.455 [2.392]	2.363(10)
M−C(10)	2.344	2.465	2.367(3)	2.466 [2.414]	2.376(8)
M−C(11)	2.347	2.464	2.326(4)	2.496 [2.392]	2.322(10)
C(1)−C(2)	1.414	1.415	1.432(5)	1.421 [1.471]	1.44(1)
C(1)−C(5)	1.414	1.415	1.399(5)	1.421 [1.471]	1.44(1)
C(2)−C(3)	1.423	1.427	1.409(5)	1.428 [1.461]	1.41(1)
C(3)−C(4)	1.399	1.401	1.385(5)	1.396 [1.414]	1.42(1)
C(4)−C(5)	1.423	1.427	1.418(5)	1.428 [1.461]	1.42(1)
C(7)−C(8)	1.401	1.405	1.391(5)	1.405 [1.421]	1.41(1)
C(7)−C(11)	1.421	1.422	1.422(5)	1.423 [1.458]	1.44(1)
C(8)−C(9)	1.421	1.422	1.408(6)	1.423 [1.458]	1.41(1)
C(9)−C(10)	1.413	1.417	1.377(6)	1.418 [1.450]	1.44(2)
C(10)−C(11)	1.413	1.417	1.422(6)	1.418 [1.450]	1.43(2)

[a] Experimental values refer to $(MeCp)_2MoO$[6g] and $(MeCp)_2WO$ (present study). [b] Calculated MP2 geometrical parameters are in brackets.

Input parameters were $D((MeCp)_2W{=}O)$ (Table 3), $D(Me_3Si-Cl)$,[34] D(W−Cl),[32b,c] and $D(WO-SiMe_3)$. It was reasonably assumed that $D(W(OSiMe_3)-Cl) \approx D(W(Cl)-Cl)$ from thermochemical results in group 4 metallocenes.[38a,40] For $D(WO-SiMe_3)$, we employ the current estimate of $D(Me_3SiO-SiMe_3)$, 136.1(4.8) kcal/mol.[41] Results are summarized in Table 4, where it can be seen that $D(W-OSiMe_3) = 65(18)$ kcal/mol. Again, the true uncertainty in this parameter is probably substantially less than that calculated by summing the component data uncertainties, and the experimental precision is excellent.

Theoretical Results. Molecular Structure. Optimized metrical parameters for Cp_2CrO (unknown), Cp_2MoO, and Cp_2WO are set out in Table 5 and compared with available crystallographic data. The agreement is good at the HF level, with the slight overestimation in M−C distances attributable to well-known effects arising from omission of correlation.[42]

(35) (a) Bullock, W. J.; Walsh, R.; King, K. D. *J. Phys. Chem.* **1994**, *98*, 2595−2601. (b) Goumri, A.; Yuan, W.-J.; Marshall, P. *J. Am. Chem. Soc.* **1993**, *115*, 2539−2540. (c) Ding, L.; Marshall, P. *J. Am. Chem. Soc.* **1992**, *114*, 5754−5758.

(36) Chase, M. W., Jr.; Davies, C. A.; Downey, J. R.; Frurip, D. J.; MacDonald, R. A.; Syverud, A. N. JANAF Thermochemical Tables. *J. Phys. Chem. Ref. Data* **1985**, *14*, Suppl. 1.

(37) (a) Dias, A. R.; Dias, P. B.; Diogo, H. P.; Galvao, A. M.; Minas de Piedade, M. E.; Martinho Simoes, J. A. *Organometallics* **1987**, *6*, 14−27. (b) Minas da Piedade, M. E.; Shaofeng, L.; Pilcher, G. *J. Chem. Thermodyn.* **1987**, *19*, 195−202.

(38) In previous thermochemical studies on group 4,[38a,b] lanthanide,[31c] and actinide[38c] cyclopentadienyl halides, we noted that $D(L_xM-X) \approx D_1(MX_{x+1})$. Application of this approach to group 6 relies on a diverse body of metal halide thermochemical data[36] of apparently variable quality. (a) Schock, L. E.; Marks, T. J. *J. Am. Chem. Soc.* **1988**, *110*, 7701−7715. (b) King, W. A.; Lanza, G.; DiBella, S.; Fragala, I. L.; Marks, T. J. Manuscript in preparation. Absolute D(M−I) bond enthalpies for $(1,3\text{-}^tBu_2Cp)_2MI_2$, M = Zr, Hf: (c) Schock, L. E.; Seyam, A. M.; Sabat, M.; Marks, T. J. *Polyhedron* **1988**, *7*, 1517−1529.

(39) Nolan, S. P.; de la Vega, R. P.; Mukerjee, S. L.; Gonzalez, A. A.; Zhang, K.; Hoff, C. D. *Polyhedron* **1988**, *16/17*, 1491−1498. D(Mo−Cl) = 72.4 kcal/mol; D(Mo−I) = 51.8 kcal/mol.

(40) In group 4, alkoxy substitution ($L_2MR_2 \rightarrow L_2M(OR')R$) enhances D(M−R) by ca. 3−4 kcal/mol.[38a] The reason appears to be stabilization of the higher metal oxidation (resistance to homolysis) by alkoxide → M π donation. This would appear less likely in a d^2 metallocene system.

(41) (a) Walsh, R. Private communication to T.J.M. (b) Becerra, R.; Walsh, R. In *The Chemistry of Organosilicon Compounds*; Rappaport, Z., Apeloig, Y., Eds.; in press.

(42) (a) Williamson, R. L.; Hall, M. B. *Int. J. Quantum Chem., Quantum Chem. Symp.* **1987**, *21*, 503−512. (b) Pierloot, K.; Persson, B. J.; Roos, B. O. *J. Phys. Chem.* **1995**, *99*, 3465−3472. (c) Lanza, G.; Fragala, I. L.; Fu, P.-F.; Marks, T. J.; Wilson, D. C.; Rudolph, P. R. *J. Am. Chem. Soc.* Manuscript in preparation.

Table 6. Selected HF Bond Lengths (Å) and Bond Angles (deg) of Cp_2MCl_2 (M = Cr, Mo, W) Complexes

	Cp_2CrCl_2	Cp_2MoCl_2		Cp_2WCl_2
	calcd	calcd	exptl	calcd
M−$Cp_{1\ (cent.)}$	1.950	2.082	1.97	2.076
M−$Cp_{2\ (cent.)}$	1.956	2.073	1.97	2.061
Cp_1−M−Cp_2	135.8	134.9	130.9	135.5
Cl(1)−M−Cl(2)	86.6	84.3	82.0(0.2)	83.7
M−Cl(1)	2.466	2.546	2.464(6)	2.539
M−Cl(2)	2.466	2.546	2.470(5)	2.539
M−C(1)	2.190	2.323	2.25(3)	2.315
M−C(2)	2.307	2.411	2.27(3)	2.406
M−C(3)	2.325	2.443	2.30(3)	2.440
M−C(4)	2.325	2.443	2.29(3)	2.440
M−C(5)	2.307	2.411	2.30(3)	2.406
M−C(7)	2.360	2.457	2.32(3)	2.463
M−C(8)	2.360	2.457	2.38(3)	2.463
M−C(9)	2.264	2.372	2.32(3)	2.357
M−C(10)	2.230	2.335	2.27(3)	2.306
M−C(11)	2.264	2.372	2.27(3)	2.357
C(1)−C(2)	1.428	1.428	1.40(5)	1.430
C(1)−C(5)	1.428	1.428	1.35(6)	1.430
C(2)−C(3)	1.385	1.398	1.30(5)	1.401
C(3)−C(4)	1.455	1.440	1.44(6)	1.437
C(4)−C(5)	1.385	1.398	1.24(6)	1.401
C(7)−C(8)	1.412	1.411	1.25(5)	1.407
C(7)−C(11)	1.408	1.416	1.47(4)	1.407
C(8)−C(9)	1.408	1.416	1.36(4)	1.420
C(9)−C(10)	1.420	1.425	1.43(3)	1.430
C(10)−C(11)	1.420	1.425	1.40(5)	1.430

Indeed, the geometry optimization for Cp_2WO using correlated wave functions (MP2) evidences generally improved agreement between experiment and theory. The trend in M−O and M−C distances on proceeding from Cr → Mo → W mirrors differences in ionic radii.[28] Efforts to optimize the conformations of the MeCp ligands revealed that Me-eclipsed configurations lie slightly higher in energy (∼0.5 kcal/mol).

Table 6 presents optimized molecular geometries for the Cp_2MCl_2 series. Only the M = Mo member of this series has been characterized crystallographically, and it can be seen that agreement between theory and experiment is favorable in view of the uncertainties in some experimental parameters[43] and the aforementioned correlation effect caveat. Indeed, the slight overestimation of Mo−C and Mo−Cl distances is consistent with other ab initio results on metal chlorides.[44] Again, metal−ligand distances parallel trends in ionic radii.[28]

Theoretical Results. Electronic Structure and Bonding. As already noted, the structure and reactivity patterns of the present metallocene oxo complexes are unusual and raise questions doubtless connected with electronic structure. The enhanced M═O nucleophilicity, elongated M−C(Cp) contacts versus typical Cp_2MX_2 complexes, and elongated M═O distances do not lend themselves to simple explanations. Thus, simple valence bond descriptions (Cp_2M^+—O^-), the earlier Xα-SW study,[6g] and the recent PES/extended Hückel analysis[7a] do not provide completely compelling rationalizations of these unusual properties.

The bonding in the present Cp_2MO complexes can be described principally in terms of perturbations of a Cp_2M fragment by the oxo ligand. In the C_s molecular symmetry dictated by the staggered MeCp rings, all oxo O_{2p} orbitals can engage in bonding, and in principle, an M≡O bond should result. Reference to the Cp_2MoO ab initio atomic population data (Table 7) suggests similar conclusions. Thus, the valence MOs can be grouped in terms of π_2-Cp[45] based (30a′, 16a″−28a′) and O_{2p} (14a″−26a′) MOs. Contour plots of the latter (Figure 2) are partly suggestive of an Mo≡O triple bond involving the $4d_{x^2-y^2}$ (σ_{Mo-O}), $4d_{yz}$, and $4d_{xy}$ (π_{Mo-O}) metal orbitals. Analogous data for the π_2-Cp-based MOs reveal no anomalies relative to other Cp_2MX_n complexes previously investigated.[46] Finally, the 29a′ MO represents the metal electrons responsible for the metal d^2 configuration. Note that this latter MO does not represent the lowest lying HOMO, in contrast to the PES results.[7b] Inclusion of relaxation effects upon ionization results in the expected disruption of the ground-state MO ordering due to the greater differential relaxation energy[47] associated with removal of a metal electron from the

Table 7. Eigenvalues and Mulliken Population Analysis of $(\eta^5\text{-}C_5H_5)_2MoO$

MO	−ϵ (eV)	ΔSCF (eV)	IE[a] (eV)	contribution metal	oxygen	$2(C_5H_5)$	dominant character
30a′	8.22	6.55	7.70	1	16	83	π_2
29a′	8.90	6.27	6.53	51	8	41	$4d_{z^2} + \pi_2$
16a″	9.35	8.27	8.4	11	2	87	$\pi_2 + 5p_z$
15a″	9.93	8.97	8.91	22	0	78	$\pi_2 + 4d_{xz}$
28a′	10.41		9.52	51	3	46	$\pi_2 + 4d_{z^2}$
14a″	12.15		10.67	26	72	2	$\pi_{Mo-O} + 4d_{yz}$
27a′	13.31			23	66	11	$\pi_{Mo-O} + 4d_{xy}$
26a′	13.57			28	64	8	$\sigma_{Mo-O} + 4d_{x^2-y^2}$

Bond orders: Mo−C (average), 0.27; Mo−O, 1.90

[a] Experimental data from ref 7a.

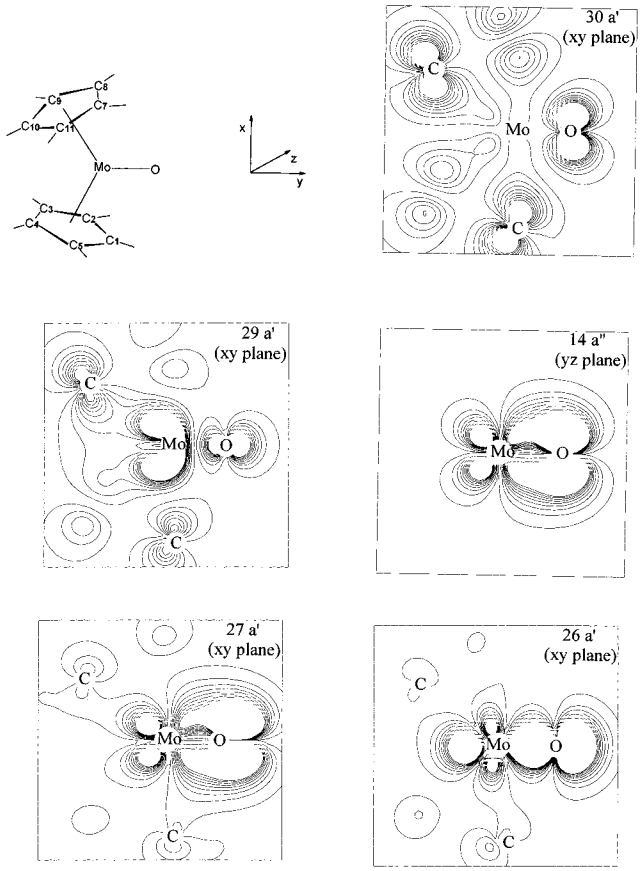

Figure 2. Electron density contour plots of the frontier MOs of $(\eta^5\text{-}C_5H_5)_2MoO$. The first contour is 0.01 e au^3, and the interval between successive contours is 0.0012 e/au^3.

(43) Prout, K.; Cameron, T. S.; Forder, R. A.; Critchiley, S. R.; Denton, B.; Rees, G. V. *Acta Crystallogr.* **1974**, *B30*, 2290−2304.

(44) (a) Lanza, G.; Fragala, I. L. *Chem. Phys. Lett.* **1996**, *255*, 341−346. (b) Williamson, R. L.; Hall, M. B. In *The Challenge of d and f Electrons*; Salahub, D. R., Zerner, M. C., Eds.; ACS Symposium Series; 1989; 394, pp 17−36.

(45) Evans, S.; Green, M. L. H.; Jewitt, A. F.; Orchard, A. F.; Pygall, C. F. *J. Chem. Soc., Faraday Trans. 2* **1972**, *68*, 1847−1865.

Table 8. Eigenvalues and Mulliken Population Analysis of $(\eta^5\text{-}C_5H_5)_2MoCl_2$

		contribution			
MO	$-\epsilon$ (eV)	metal	2Cl	2(C_5H_5)	dominant character
30a′	9.18	44	50	6	$4d_{z^2} + \pi_{Cl}$
29a′	9.33	9	49	42	$\pi_2 + \pi_{Cl} + 4d_{xy}$
19a″	9.54	1	83	16	πCl
18a″	9.76	5	71	24	$\pi_{Cl} + 4d_{xz}$
17a″	10.65	16	16	68	$\pi_2 + 4d_{yz}$
16a″	11.06	18	77	5	$\sigma_{Mo-Cl} + 4d_{yz} + 5p_z$
28a′	11.23	20	19	61	$\pi_2 + 4d_{x^2-y^2} + 5p_y$
27a′	11.46	31	66	3	$\sigma_{Mo-Cl} + 5s + 4d_{x^2-y^2}$
26a′	11.59	22	45	33	$\pi_{Cl} + 4d_{xy}$
15a″	11.62	23	25	52	$\pi_2 + 4d_{xz}$
25a′	11.96	46	39	15	$\pi_{Cl} + 4d_{z^2}$
bond orders: Mo−C (average), 0.35; Mo−Cl, 1.08					

d^2 configuration. Furthermore, analysis of the population data provides an indication of additional intriguing details.

Note that the metal-based 29a′ MO has a sizable contribution from the O_{2p} and Cp-based MOs. The contour plot analysis indicates that it possesses M−O antibonding character due to four-electron/two-orbital interactions involving the 26a′ and 29a′ MOs (Figure 2). This effect is clearly associated with a reduced M−O bond order. In contrast, the Cp contribution is associated with M → Cp back-donation effects since the contour plot in the plane parallel to the Cp ring reveals the characteristic nodal properties of empty π_3-Cp orbitals. The ab initio analysis of the Cp-related MOs warrants further comments. The 16a″, 15a″, and 28a′ MOs are almost totally metal−Cp in character without significant O_{2p} contributions. In contrast, the 30a′ MO has a significant O_{2p} contribution due to repulsive interligand intramolecular interactions.

Photoelectron spectra of the present oxo complexes have been recorded and analyzed at Catania and reveal neither new details nor discrepancies from those recorded at Oxford.[7a] In particular, the spectra provide strong experimental support for the present ab initio MO energy sequence as well as for the 1:3 grouping of π_2-Cp-related ionizations. On the basis of extensive theoretical and PES studies of Cp_2ML_n complexes,[46a] the MO sequences have been operationally divided into three categories: classes A and C where the π_2-Cp-based MOs lie higher or lower in energy, respectively, relative to the L-based MOs, and class B where the two sets lie close in energy and are strongly admixed. The present oxo complexes clearly belong to class A, and as a consequence, the aforementioned repulsive O−Cp interligand interactions effect some antibonding destabilization of the π_2-Cp orbitals. In the same context, note that on the basis of the present ab initio populations (Table 8) as well as upon earlier experimental PES data,[46a] $(MeCp)_2MoCl_2$ unequivocally belongs to class C. Thus, the corresponding interligand repulsive effects stabilize the Cp-based MOs.

Depending on the MO ordering class, charge can be either withdrawn from the Cp rings to other ligands (class A) or released to the Cp ligands (class C). In class A complexes, minor charge remains for Cp−M bonding which is necessarily weakened. In terms of metrical parameters, a clear shortening of the M−C(Cp) distances is observed upon proceeding from Cp_2MoO (2.369(3) Å) to Cp_2MoCl_2 (2.30(1) Å) and from $(MeCp)_2WO$ (2.371(8) Å) to $[(Me_5Cp)(CO)(NO)Re(\mu_2\text{-}\eta^3\text{-}CO_2)WCp_2]^+BF_4^-$ (2.30 Å).[6b] Similar conclusions can be reached by inspection of ab initio M−C bond orders on passing from the oxo to the parent chloride complexes (Table 7) where smaller values are associated with the former. Interestingly, the M−O bond orders are almost twice the M−Cl bond orders, as expected on passing from a single to a double bond, providing clear evidence of the aforementioned 29a′ MO antibonding character. Note also that the calculated M−Cp(centroid) bond lengths in the $Cp_2M(OSiH_3)Cl$ series (Cr, 1.98; Mo, 2.11; W, 2.10 Å) are intermediate between the corresponding Cp_2MO and Cp_2MCl_2 values. This result is consistent with progressive, interligand repulsion-induced destabilization of the metal−ring bonding as chloride is replaced by oxygenate ligands.

Table 9. Calculated M═O and M−O Dissociation Energies for the $Cp_2M{=}O/Cp_2M(OSiH_3)Cl$ Series (M = Cr, Mo, W) in Kcal/Mol.

	D(M═O)					D(M−O)[b]		
M	HF	MP2	MP3	MP4(SDQ)	exptl	HF	MP2	exptl
Cr	−23.2	140.1	35.8	161.3		48.5	52.2	
Mo	14.3	143.1	81.5	130.3	111	25.4	58.2	
W	45.3	153.2	107.2	140.9	132	42.4	67.9	65

[a] Derived from $Cp_2M{=}O \rightarrow Cp_2M + O$. [b] Derived from $Cp_2MO + SiH_3Cl \rightarrow Cp_2MCl(OSiH_3)$.

The nucleophilic character of the Cp_2MO complexes,[6] as well as other reactivity patterns, is in good agreement with the substantial electronic charge accumulation in the space volume surrounding the oxo ligand. As a probe of the oxo ligand nucleophilicity, proton affinities (eq 15)

$$Cp_2MO + H^+ \rightarrow \underset{\mathbf{C}}{Cp_2MOH^+} \qquad (15)$$

were computed at theMP2 level, yielding $\Delta H^{rxn} = -235$, -226, and -227 kcal/mol for Cp_2CrO, Cp_2MoO, and Cp_2WO, respectively. In comparison, the computed proton affinities for NH_3 and PH_3 at a similar level of theory are -219 and -197 kcal/mol, respectively, indicating appreciably greater basicity for the oxo complexes. Interestingly, the calculated O−H bond lengths in **C** are independent of metal (0.94 Å) while the M═O elongation is greater for Cr (+0.22 Å) than for Mo and W (+0.15, +0.13 Å, respectively) in accord with the greater computed Cp_2CrO basicity.

Theoretical Results. Bond Dissociation Energies. Calculated M═O bond dissociation enthalpies are compiled in Table 9. It can be seen that D(M═O) parameters are significantly, and not unexpectedly,[7b,c] underestimated at the HF level (Cp_2CrO is predicted to be unbound). Thus, the inclusion of correlation effects, through MP2 procedures, results in bound states, the BDE values of which are in reasonable agreement with thermochemical data. Changes of correlation energy associated with molecule formation represent the major stabilizing effect in the present complexes. Effects due to high-order correlation effects have been tested through the MP3 and MP4(SDQ) procedures. At the MP3 level, a substantial falloff in total dissociation energy values (relative to MP2) is observed. The effect appears more pronounced for Cp_2CrO, and in all cases leads to poor agreement with experiment. On passing to the MP4(SDQ) level, smaller (∼10 kcal/mol relative to MP2)

(46) (a) Cauletti, C.; Clark, J. P.; Green, J. C.; Jackson, S. E.; Fragala, I.; Ciliberto, E.; Coleman, A. W. *J. Electron Spectrosc. Relat. Phenom.* **1980**, *18*, 61−73. (b) Casarin, M.; Ciliberto, E.; Gulino, A.; Fragala, I. *Organometallics* **1989**, *8*, 900−906. (c) Ciliberto, E.; Di Bella, S.; Gulino, A.; Fragala, I.; Petersen, J. L.; Marks, T. J. *Organometallics* **1992**, *11*, 1727−1737. (d) Di Bella, S.; Gulino, A.; Lanza, G.; Fragala, G.; Marks, T. J. *Organometallics* **1993**, *12*, 3326−3332. (e) Di Bella, S.; Gulino, A.; Lanza, G.; Fragala, I.; Stern, D.; Marks, T. J. *Organometallics* **1994**, *13*, 3810−3815.

(47) (a) Kozlowski, P. M.; Davidson, E. R. *Chem. Phys. Lett.* **1994**, *222*, 615−620. (b) Siegbahn, P. E.; Svensson, M. *Chem. Phys. Lett.* **1993**, *216*, 147−154. (c) DiBella, S.; Lanza, G.; Gulino, A.; Fragala, *I. Inorg. Chem.* **1996**, *35*, 3885−3890.

BDEs are observed for both Mo and W, in close agreement with experimental data. In the case of Cp_2CrO, in contrast, a substantial increase of the BDE energy is observed. This observation clearly indicates that the MP*n* series is reasonably converged at the MP4 level for both Mo and W metallocenes and, in turn, represents a useful tool for predicting metallocene bond dissociation enthalpies. In contrast, a marked fluctuation in computed D(Cr═O) values is found for Cp_2CrO. This is a common feature for first-row transition element complexes due to the poor description of interelectronic repulsion terms by single-determinant wave functions.[47] In these cases, higher level treatments are clearly required.[47] In regard to computation of M—O single bond energies, it can be seen in Table 9 that agreement between theory and experiment is good, even at the MP2 level. It is noteworthy that the calculated values of both D(M═O) and D(M—O) exhibit significant increases upon descending the Periodic Table.

Discussion

Synthesis and Molecular Structure. The present results demonstrate efficient, straightforward, high-yield synthetic routes to a variety of Cp_2MH_2-, Cp_2MCl_2-, and Cp_2MO-type complexes. Such complexes should now be available in greater quantities for experimentation. The present molecular structure results for $(MeCp)_2WO$ evidence characteristics vis-à-vis Cp_2WX_2 analogues in common with those previously noted for the Mo congeners: elongated metal—Cp bonding contacts and metal—oxo distances which are longer than expected.

Bonding and Bonding Energetics. The foregoing electronic structure analysis provides a convincing quantitative rationalization of weakened M—Cp bonding (charge withdrawal; interligand repulsion), weakened M═O bonding (population of M—O antibonding levels), and nucleophilic character (substantial negative charge accumulation on the oxo functionality). This analysis is accompanied by calculated molecular metrical parameters and bond dissociation enthalpies which are in favorable agreement with experiment.

The present thermochemical results represent, to our knowledge, some of the first D(M═O) data for organometallic complexes.[48] It can be seen that the experimental $D(MeCp)_2$M═O values are large, with the ~20 kcal/mol increase on proceeding from Mo to W, typical of second-row versus third-row metal—ligand bond dissociation enthalpy patterns[32b,49,50] and usually explained in terms of orbital overlap and promotion energy effects.[49,50] The present experimental data compare favorably to D(M═O) values of 96 kcal/mol in $(Et_2NCS_2)_2Mo({=}O)_2$,[3b] 141(9) kcal/mol in $(Me_3tacn)ReCl_2({=}O)^+$,[3a] 117 kcal/mol in $(Me_5Cp)ReO_3$,[48] and 90(1) kcal/mol in $(Me_5Cp)_2(PhCH_2O)U{=}O$.[51] The present metallocene D(M═O) values as well as Mo → W trends are also roughly in the range reported for the gaseous M^{VI} oxohalide pair $MoCl_4O$ (101 kcal/mol) and WCl_4O (127 kcal/mol);[1c] however, the magnitudes are substantially lower than in the gaseous diatomics MoO (133.9 kcal/mol) and WO (160.6 kcal/mol), which presumably have metal—oxygen triple bonds.[52] Interestingly, the expected 4d vs 5d trend is apparently not observed for D_1(M═O) in gaseous MoO_3 (151 kcal/mol) and WO_3 (152 kcal/mol).[1c] These relationships are summarized in Table 10.

Table 10. Comparison of Group 6 Metal—Oxo Bond Dissociation Enthalpies (kcal/mol)

$(MeCp)_2MoO$	110^a	$(MeCp)_2WO$	132^a
$MoCl_4O$	101^b	WCl_4O	127^b
MoO_3	151^b	WO_3	152^b
MoO	134^c	WO	160^c
$(Et_2NCS_2)_2MoO_2$	96^d		

^{a} This work. ^{b} From ref 1c. ^{c} From ref 39. ^{d} From ref 3b.

The present $D(W{-}OSiMe_3)$ value, 65(18) kcal/mol, represents, to our knowledge, the first group 6 metallocene alkoxy bond enthalpy determined. It is somewhat smaller in magnitude then those for analogous Cp_2W carboxylates (~83 kcal/mol)[32c] and $Cp_2Hf(OC_6F_5)_2$ (98(3) kcal/mol).[38a]

Chemical Implications. The present D(M═O)/D(M—O) bond enthalpy results provide thermochemical insight into the course of a number of reported and potential Cp_2MO-centered reactivity patterns. In many cases a delicate balance in M═O versus M—O bonding energetics appears crucial in dictating reaction pathways. In the analyses which follow, existing group 6 Cp_2MX_2 bond enthalpy data,[32a,b,53] strain enthalpy data,[54] and tabulated small molecule bond enthalpy data[55] are employed. We assume, for the present purposes, that $(Me_5Cp)_2M$— and $(MeCp)_2M$— thermochemical parameters are approximately transferable. The estimated uncertainty in calculated enthalpies is probably on the order of about ±8 kcal/mol.

In regard to processes which transfer the oxo ligand, the present results indicate that direct transfer[56] to substrates such as olefins (to effect epoxidation) is highly endothermic by virtue of the strong metal—oxo bonding (eq 16). For the same reasons,

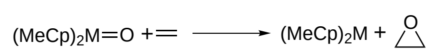

(16)

$$\Delta H_{calcd} \approx +29 \text{ kcal/mol, M} = \text{Mo}$$

$$\Delta H_{calcd} \approx +51 \text{ kcal/mol, M} = \text{W}$$

(48) (a) D(Re═O) in $(Me_5Cp)ReO_3$ has recently been measured relative to $[(Me_5Cp)ReO]_2(\mu\text{-}O)_2$(toluene) ⇌ $2(Me_5Cp)ReO_2$(toluene) by Ph_3P abstractive calorimetry.[48b] D(Re═O) was estimated to be 116.8(1.2) kcal/mol. (b) Gable, K. P.; Juliette, J. J.; Li, C.; Nolan, S. P. *Organometallics* **1996**, *15*, 5250—5251.

(49) (a) Martinho Simoes, Ed. *Energetics of Organometallic Species*; Kluwer: Dordrecht, 1992; see also references therein. (b) Hoff, C. D. *Prog. Inorg. Chem.* **1992**, *40*, 503—561. (c) Marks, T. J., Ed. *Bonding Energetics in Organometallic Compounds;* ACS Symposium Series, American Chemical Society: Washington, DC, 1990; p 428.

(50) (a) *Metal—Ligand Bonding Energetics in Organotransition Metal Compounds*; Marks, T. J., Ed.; Polyhedron Symposium-in-Print; 1988; Vol. 7. (b) Skinner, H. A.; Connor, J. A. *Pure Appl. Chem.* **1985**, *57*, 79—88 (c) Pilcher, G.; Skinner, H. A. In *The Chemistry of the Metal—Carbon-Bond;* Harley, F. R., Patai, S., Eds; Wiley: New York, 1982; pp 43—90.

(51) King, W. A.; Arney, D. S. J.; Burns, C. J.; Marks, T. J. Unpublished results.

(52) Pedley, J. B.; Marshall, E. M. *J. Phys. Chem. Ref. Data* **1984**, *12*, 967—971.

(53) In cases where only a single D(M—ligand) datum is available for a Mo, W pair, the

$$\frac{D(\text{Mo}-\text{CH}_3)}{D(\text{W}-\text{CH}_3)} = \frac{D(\text{Mo}-\text{ligand})}{D(\text{W}-\text{ligand})}$$

proportionality is employed. It is assumed that metal substituent effects on bond enthalpies attenuate in two bonds.

(54) (a) Organic molecules: Isaacs, N. S. *Physical Organic Chemistry;* Wiley: New York, 1987; pp 282—291. (b) Metallacyclobutanes: Bruno, J. W.; Marks, T. J.; Morss, L. R. *J. Am. Chem. Soc.* **1983**, *105*, 6824—6832.

(55) (a) Griller, D.; Kanabus-Kaminska, J. M.; Maccoll, A. *J. Mol. Struct.* **1988**, *163*, 125—131. (b) Pedley, J. B.; Naylor, R. D.; Kirby, S. P. *Thermochemical Data of Organic Compounds*, 2nd ed.; Chapman and Hall: London, 1986; Appendix Tables 1 and 3. (c) McMillan, D. F.; Golden, D. M. *Annu. Rev. Phys. Chem.* **1982**, *33*, 493—532 and references therein. (d) Benson, S. W. *Thermochemical Kinetics*, 2nd ed.; John Wiley and Sons: New York, 1976; Appendix Tables A.10, A.11, and A.22. (d) Benson, S. W. *J. Chem. Educ.* **1965**, *42*, 502—518.

(56) For non-metallocene examples where this pathway is thought to be operative, see: (a) Zhang, W.; Lee, N. H.; Jacobsen, E. N. *J. Am. Chem. Soc.* **1994**, *116*, 425—426 and references therein. (b) Fu, H.; Look, G. C.; Zhang, W.; Jacobsen, E. N.; Wong, C.-H. *J. Org. Chem.* **1991**, *56*, 6497—6502. (c) Groves, J. T.; Stern, M. K. *J. Am. Chem. Soc.* **1988**, *110*, 8628—8638.

it is therefore not surprising that photogenerated Cp_2W reacts with propylene oxide to produce Cp_2WO (the reverse of eq 16).[6g,i] The large endothermicity of eq 16 can be compensated by reoxygenation (eq 17), with the eq 16 + eq 17 enthalpic

$$(MeCp)_2M + {}^1/_2O_2 \rightarrow (MeCp)_2M{=}O \qquad (17)$$

$$\Delta H_{calcd} \approx -51 \text{ kcal/mol, M} = \text{Mo}$$

$$\Delta H_{calcd} \approx -73 \text{ kcal/mol, M} = \text{W}$$

sums of −22 (M = Mo) and −22 (M = W) kcal/mol in favorable agreement with the enthalpy of oxygenation of ethylene to ethylene oxide calculated from standard heats of formation (−25.1 kcal/mol; an internal consistency check).[55] The endothermicity of eq 16 can also be partially compensated by binding[32a] of a substrate molecule (eq 18).

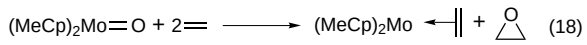

(18)

$$\Delta H_{calcd} \approx +15 \text{ kcal/mol}$$

Alternative epoxidation scenarios include oxo → metallaoxirane [2 + 2] cycloaddition processes.[57] For the present metallocene complexes, such processes are estimated to be slightly exothermic (eq 19); the favorable formation of the M−C

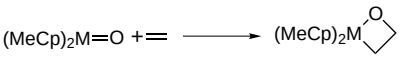

(19)

$$\Delta H_{calcd} \approx -3 \text{ kcal/mol, M} = \text{Mo}$$

$$\Delta H_{calcd} \approx -7 \text{ kcal/mol, M} = \text{W}$$

and M−O bonds is counterbalanced by the loss of the strong M=O bond. Such processes are likely endergonic at room temperature (2 particles → 1 particle), and to our knowledge have not been observed.[4−6,58] Coupling eq 19 with ethylene oxide reductive elimination also involves a highly endothermic process for the present metallocenes (eq 20).

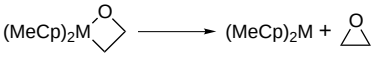

(20)

$$\Delta H_{calcd} \approx +32 \text{ kcal/mol, M} = \text{Mo}$$

$$\Delta H_{calcd} \approx +58 \text{ kcal/mol, M} = \text{W}$$

Equation 19 typifies a [2 + 2] cycloaddition reactivity pattern which is common for groups 4 and 6 metallocene oxo complexes, but as noted above has not been reported for simple olefins. The thermochemical data argue that the strengths of the M−O and M−C bonds formed are insufficient to overcome the large M=O bond enthalpy and anticipated ring strain.[54b,59] However, in the case of acetylenic reagents, cycloaddition is calculated to be significantly more exothermic than for ethylene (eq 21). The former trend likely reflects the generally greater

(21)

$$\Delta H_{calcd} \approx -20 \text{ kcal/mol, M} = \text{Mo}$$

$$\Delta H_{calcd} \approx -25 \text{ kcal/mol, M} = \text{W}$$

exothermicity of additions to acetylenes[60] as well as the stronger metal−vinyl bond[32a,b,53] which is formed. Equation 21 has considerable precedent in group 4 chemistry.[4] The cycloaddition of ketones to oxometallocenes (eq 22) benefits from the

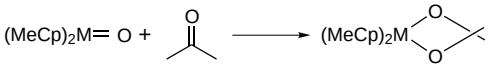

(22)

$$\Delta H_{calcd} \approx -1 \text{ kcal/mol, M} = \text{Mo}$$

$$\Delta H_{calcd} \approx -11 \text{ kcal/mol, M} = \text{W}$$

formation of two relatively strong M−O bonds but is less exothermic due to the loss of the strong ketonic C=O bond. Both reversible and irreversible cycloadditions of ketones have been observed for $Cp_2W{=}O$,[6b] which is consistent with the above thermochemical estimates.

Reactions of oxo complexes with hydrogen donors offer the potential for both deoxygenation (eqs 23 and 24, assuming D(MO−H) ≈ D(MeO−H)) as well as for saturated hydrocarbon functionalization (eqs 25 and 26). The overall result of the eqs

$$(MeCp)_2M{=}O + H_2 \rightarrow (MeCp)_2M(H)OH \qquad (23)$$

$$\Delta H_{calcd} \approx -14 \text{ kcal/mol, M} = \text{Mo}$$

$$\Delta H_{calcd} \approx -21 \text{ kcal/mol, M} = \text{W}$$

$$(MeCp)_2M(H)OH + H_2 \rightarrow (MeCp)_2MH_2 + H_2O \qquad (24)$$

$$\Delta H_{calcd} \approx -13 \text{ kcal/mol, M} = \text{Mo}$$

$$\Delta H_{calcd} \approx -10 \text{ kcal/mol, M} = \text{W}$$

$$(MeCp)_2M{=}O + CH_4 \rightarrow (MeCp)_2M(H)OCH_3 \qquad (25)$$

$$\Delta H_{calcd} \approx +8 \text{ kcal/mol, M} = \text{Mo}$$

$$\Delta H_{calcd} \approx +1 \text{ kcal/mol, M} = \text{W}$$

$$(MeCp)_2M{=}O + CH_4 \rightarrow (MeCp)_2M(CH_3)OH \qquad (26)$$

$$\Delta H_{calcd} \approx +5 \text{ kcal/mol, M} = \text{Mo}$$

$$\Delta H_{calcd} \approx 0 \text{ kcal/mol, M} = \text{W}$$

23 and 24 sequence has been reported for $(Me_5Cp)_2W{=}O$ at

(57) (a) Kolb, H. C.; Van Nieuwenhze, M. S.; Sharpless, K. B. *Chem. Rev.* **1994**, *94*, 2483−2547. (b) Sundermeyer, J. *Angew. Chem., Int. Ed. Engl.* **1993**, *32*, 1144−1146. (c) Jorgensen, K. A.; Schiott, B. *Chem. Rev.* **1990**, *90*, 1483−1506. (d) Mimoun, H. In *Comprehensive Coordination Chemistry*; Wilkinson, G., Gillard, R. D., McCleverty, J. A., Eds.; Pergamon: Oxford, 1987; Chapter 61.3.

(58) The adverse $T\Delta S$ contribution to ΔG under these conditions is likely on the order of ∼4−8 kcal/mol owing to loss of translational and rotational entropy: (a) Smith, G. M.; Carpenter, J. D.; Marks, T. J. *J. Am. Chem. Soc.* **1986**, *108*, 6805−6807. (b) Menger, F. M.; Venkataram, U. V. *J. Am. Chem. Soc.* **1985**, *107*, 4706−4709 and references therein. (c) Page, M. I. In *The Chemistry of Enzyme Action;* Page, M. I., Ed.; Elsevier: New York, 1984; pp 1−54. (d) Kirby, A. *Adv. Phys. Org. Chem.* **1980**, *17*, 183−278.

(59) Interestingly, Andersen[4b] has observed a Ti=O cycloaddition reaction with allene, and thermochemical estimates for group 6 $(MeCp)_2M{=}O$ complexes yield ΔH_{calcd} vales of −23 (M = Mo) and −27 (M = W) kcal/mol for formation of such an oxametallacycle:

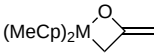

This reflects the generally greater exothermicity of additions to allenes.

(60) (a) Li, Y.; Marks, T. J. *J. Am. Chem. Soc.* **1996**, *118*, 9295−9306. (b) Li, Y.; Marks, T. J. *Organometallics* **1996**, *15*, 3770−3772. (c) Li, Y.; Fu, P.-F.; Marks, T. J. *Organometallics* **1994**, *13*, 439−440.

high temperatures,[6e] and the principal driving force is seen to be the formation of strong O—H bonds. Interestingly, methane activation by the present metallocene oxo complexes (eqs 25 and 26) is not estimated to be as exothermic as eq 24, primarily because the energetic demands of C—H scission are not compensated in this case by the formation of a particularly strong C—O bond.

In regard to catalytic hydrocarbon oxidation, eq 27 embodies some aspects of proposed propene → acrolein oxidative scenarios.[57b,61] The process is estimated to be endothermic, the

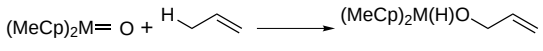

(27)

$$\Delta H_{calcd} \approx +5 \text{ kcal/mol, M} = \text{Mo}$$

$$\Delta H_{calcd} \approx -2 \text{ kcal/mol, M} = \text{W}$$

weaker reactant C—H bond vs eq 26 counterbalanced by a weaker product C—O bond. However, it can also be seen that transfer of the propylene hydrogen to an adjacent oxo functionality[57b,61] with stronger O—H bonding than to a metal center would likely render the process exothermic. For both eqs 25 and 27, subsequent β-H elimination of the alkoxy fragment is estimated to be endothermic, so that overall H_2/O transposition is endothermic, due to the substantial strength of the M═O bonds (e.g., eq 28). Furthermore, coupling eqs 25

$$(MeCp)_2M{=}O + CH_4 \rightarrow (MeCp)_2MH_2 + CH_2O \quad (28)$$

$$\Delta H_{calcd} \approx +28 \text{ kcal/mol, M} = \text{Mo}$$

$$\Delta H_{calcd} \approx +21 \text{ kcal/mol, M} = \text{W}$$

and 26 to hydrogenolytic processes is also calculated to be endothermic (eq 29).

$$(MeCp)_2M{=}O + CH_4 + H_2 \rightarrow (MeCp)_2MH_2 + CH_3OH \quad (29)$$

$$\Delta H_{calcd} \approx +10 \text{ kcal/mol, M} = \text{Mo}$$

$$\Delta H_{calcd} \approx +6 \text{ kcal/mol, M} = \text{W}$$

Finally, group 6 metallocene oxo complexes are also reported to undergo reversible aquation,[6e] and in accord with these observations, the thermodynamic analysis indicates that H_2O addition processes are slightly exothermic (eq 30). In contrast,

$$(MeCp)_2M{=}O + H_2O \rightleftharpoons (MeCp)_2M(OH)_2 \quad (30)$$

$$\Delta H_{calcd} \approx -1 \text{ kcal/mol, M} = \text{Mo}$$

$$\Delta H_{calcd} \approx -11 \text{ kcal/mol, M} = \text{W}$$

alkylation processes[62] which capitalize on the nucleophilicity of the oxo ligand are estimated to be more exothermic (eq 31).

$$(MeCp)_2M{=}O + CH_3I \rightarrow (MeCp)_2M(I)OCH_3 \quad (31)$$

$$\Delta H_{calcd} \approx -29 \text{ kcal/mol, M} = \text{Mo}$$

$$\Delta H_{calcd} \approx -37 \text{ kcal/mol, M} = \text{W}$$

Conclusions

The present results indicate that the electronic structure of group 6 $(MeCp)_2MO$ complexes falls within the general bonding patterns of other early transition metal metallocenes, with the elongated M—Cp and M═O bonds as well as the oxo nucleophilicity readily and quantitatively understandable. The present M═O and M—O bonds are nevertheless rather strong, and the oxo chemistry is dominated by addition processes which preserve M—O bonding. Complete M═O bond scission is driven only by processes which form very strong product bonds to oxygen (e.g., Si—O and H—O). The generality of these electronic structural and thermochemical patterns is presently under investigation.

Acknowledgment. This research was supported by the U.S. National Science Foundation (T.J.M., L.L., Grant CHE-961889), the Ministero dell Universitá e della Ricerca Scientifica e Tecnologica (G.L., I.L.F., MURST, Rome), and the Consiglio Nazionale delle Ricerche (G.L., I.L.F., CNR, Rome). The CINECA computer center (Casalecchio di Reno, BO, Italy) is also gratefully acknowledged for providing a grant of computer time.

Supporting Information Available: Diagram of the apparatus for $Cp_2MH_2/(MeCp)_2MH_2$ synthesis and crystal structure report for $(MeCp)_2WO$ (14 pages). See any current masthead page for ordering information and Web access instructions.

JA971010B

(61) Moro-Oka, Y.; Ueda, W. *Adv. Catal.* **1994**, *40*, 233−273.

(62) Interestingly, $(Me_5Cp)_2W{=}O$ is reported to yield $(Me_5Cp)_2W(O)CH_3^+I^-$ in this reaction.[6e]